

TRULY 3D MIDSAGITTAL PLANE EXTRACTION FOR ROBUST NEUROIMAGE REGISTRATION

Leonid Teverovskiy and Yanxi Liu

Carnegie Mellon University

ABSTRACT

This paper describes a robust algorithm for reliable Midsagittal Plane extraction (iMSP) from 3D neuroimages. The algorithm makes no assumptions about initial orientation of a given 3D brain image and works reliably on neuroimages of normal brains as well as brains with significant pathologies. Presented technique is truly three-dimensional since we treat each neuroimage as a three-dimensional volume rather than a set of two-dimensional slices. We use an edge-based approach which employs cross-correlation to extract iMSP. Proposed algorithm was quantitatively evaluated on a variety of real and artificial neuroimages. We find that our algorithm is able to extract iMSP from neuroimages with arbitrary initial orientations, large asymmetries, and low signal to noise ratio. We also demonstrate that presented algorithm can increase robustness of existing neuroimage registration algorithms, be it rigid, affine or less restricted deformable registration. Our algorithm was implemented using Insight Toolkit(ITK).

1. INTRODUCTION

In many neuroimage processing and classification tasks [10, 9] it is important to know the location of the midsagittal plane. Such tasks include statistical quantification of human brain asymmetry [4, 5, 15], exploring changes in brain asymmetry due to aging or a disease, classification tasks where symmetry-based features are used for discrimination between groups of people. Knowing midsagittal plane can also be useful in the process of registering neuroimages because it allows roughly pre-align the images and also reduces the number of transformation parameters which registration process has to estimate. Another possible application of the midsagittal plane extraction algorithm is in bringing neuroimages into standard coordinate system, like commonly used Talairach coordinate system [14], automatically. Talairach framework relies on landmarks and defines principal orthogonal coordinate axes based on interhemispheric midsagittal plane, AC-PC line¹ and VAC line². However, in some normal brains and in many pathological brains with tumors or lesions interhemispheric midsagittal plane is not a geometric plane but a curved two-dimensional surface. In such cases, therefore, the coordinate axis based on interhemispheric midsagittal plane in Talairach coordinate system is defined ambiguously. This ambiguity

This work is partially supported by NIH grants R21 DA015900-01, MH064625, MH01077, AG05133.

¹line passing through the superior aspect of the anterior commissure (AC) and the inferior aspect of the posterior commissure (PC)

²line passing through the posterior margin of anterior commissure and perpendicular to AC-PC line

can be removed by defining an *ideal midsagittal plane* (iMSP) as a virtual geometric plane about which the three-dimensional anatomical structure captured in the given neuroimage exhibits maximum bilateral symmetry [10]. Fully automatic extraction of iMSP presents a number of challenges posed by various extrinsic and intrinsic factors. These factors include initial orientation of the neuroimage, the amount of noise present and the degree of asymmetry of the input neuroimage. In this paper we propose a simple algorithm that can quickly and accurately estimate iMSP in neuroimages. We demonstrate that the algorithm performs well no matter whether the neuroimage is represented by a set of axial, coronal, sagittal or arbitrarily oriented slices. We show that the algorithm is robust to the presence of strong noise in the image or large tumors. The paper is organized as follows. Section 2 reviews existing work on automatic MSP extraction. Section 3 describes proposed algorithm for automatic ideal midsagittal plane extraction. Section 4 contains quantitative evaluation of the algorithm's performance when applied to normal, highly asymmetric and noisy neuroimages. Section 5 illustrates advantages of using the algorithm as a preprocessing step of registration process, and, finally, in section 6 we present our conclusions.

2. RELATED WORK

Existing MSP extraction algorithms can be divided into 2 conceptually different groups. First group of algorithms defines MSP in terms of anatomical structures of the brain [2]. Such methods assume that the interhemispheric fissure of the brain is approximately planar and is, in fact, a good approximation to MSP. Therefore, they identify task of estimating MSP with the task of detecting the interhemispheric fissure. Once the fissure is found, its location is used to estimate MSP. The fact that interhemispheric fissure is often not planar even in normal brains limits robustness of this kind of approaches. Also, such algorithms are sensitive to modality of the image, image artifacts, and often require segmentation as a preprocessing step. The other group of techniques defines MSP as a symmetry plane of a neuroimage [1, 6, 10]. Methods in this group usually define a symmetry measure and find a plane which maximizes it. Depending on the type of symmetry measure and whether it is applied to the original intensity image or to a volume that was preprocessed, the algorithms in this group can be affected by the global asymmetry of the brain. This is because if the brain is significantly tilted, corresponding left and right anatomical structures of the brain do not appear on the same slice. Consequently, symmetry lines which are computed on each 2D slice are meaningless and lead to erroneous estimations of MSP. 3D methods that compute symmetry measure on the entire volume have the potential of overcoming the neuroimage orienta-

tion constraint of 3D slice based algorithms. A different approach is employed by Prima, et al [13]. They utilize deformable registration and block matching to compute MSP. However, they report that their approach breaks if the yaw and roll angles of the given neuroimage are about 21 degrees [13]. This is approximately the same as the breaking point reported by Liu et al [10] for their algorithm where midsagittal plane was estimated from a set of 2D slices.

3. IDEAL MIDSAGITTAL PLANE EXTRACTION ALGORITHM

In this section we present an algorithm for extracting ideal midsagittal plane from an *arbitrarily* oriented three-dimensional neuroimage represented by a set of two-dimensional slices. In order to describe our algorithm we will first describe preprocessing operations we perform on the input neuroimage, then we specify three general components of our algorithm: our parametrization of the space of possible solutions, the metric to evaluate candidate solutions, and the exploration strategy for this parametrized space.

In order to increase robustness of our algorithm, we must reduce its sensitivity to such factors as noise, and local asymmetries of the brain. We achieve this goal by anisotropic smoothing, subsampling and edge detection [3]. Subsampling makes our algorithm insensitive to minor asymmetries of the brain. Anisotropic smoothing reduces noise in the image while preserving edges. Finally, edge detection reduces effects of the remaining noise and bias field and forces our algorithm to consider only main structures in the brain. In addition, edge detection allows us to use computationally effective measure of symmetry.

In our problem of extracting ideal midsagittal plane, the space of possible solutions is a set of all possible planes. We can define any plane by a point \mathbf{P} on the plane and a unit normal vector \vec{V} . The parametrization we use indexes the space of candidate midsagittal planes by the coordinates of point \mathbf{P} and unit vector \vec{V} . We traverse the space in the following manner.

Given \vec{V} we will change the coordinates of \mathbf{P} by \vec{V} at a time. This corresponds to moving a plane by 1 unit at a time in the direction perpendicular to the plane. Moreover, since we are looking for the plane of symmetry, we will require that candidate planes be close to the centroid of the given neuroimage. Thus, given \vec{V} , we will only consider a relatively small set of planes located near centroid that are perpendicular to \vec{V} . However, we cannot impose any restrictions on \vec{V} since we make no assumptions about initial orientation of the neuroimage. To visualize the search strategy we employ, imagine that the unit vector \vec{V} is at the center of a unit sphere. Then to consider all possible values for \vec{V} means to sweep the entire surface of the sphere with the endpoint of \vec{V} . We will embed a lattice into the surface of the sphere and visit only nodes of this lattice. Moreover we can eliminate half of the sphere from the consideration because \vec{V} and $-\vec{V}$ specify the same orientation of the plane perpendicular to them. Thus, each visited node corresponds to a particular orientation of \vec{V} . Fixing \vec{V} , we now change \mathbf{P} as described above, and retrieve the plane with the maximum correlation score computed according to (2) described below. In such a way we can assign a score to each of the \vec{V} 's. In order to make our algorithm more robust to spurious matches, we choose \vec{V} 's with three highest scores rather than a single

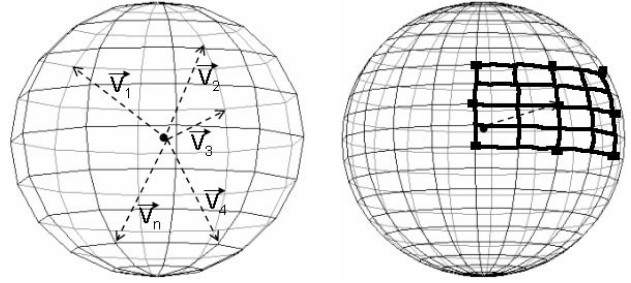


Fig. 1. We embed a coarse lattice (left) on the surface of a unit sphere and make the endpoint of \vec{V} visit every node of it. A finer lattice is embedded and explored around each of the best 3 orientations of \vec{V} .

\vec{V} with the highest score for further exploration. For each selected \vec{V} we embed a finer lattice around the node which corresponds to it and then visit every node of that finer lattice. For each of the finer lattices we pick a node with the highest score and subsequently choose the node which gives the highest score as evaluated on the full size edge image. After that we embed yet another even finer lattice around the selected node and evaluate the nodes of the lattice according to the formula (2) as applied to full sized edge image. The evaluation of the finest lattice produces \vec{V} and \mathbf{P} that correspond to the ideal midsagittal plane.

Given a particular instantiation of the point \mathbf{P} and the unit normal vector \vec{V} , we evaluate how symmetric the input neuroimage is with respect to the plane specified by these \mathbf{P} and \vec{V} using correlation of original neuroimage and its flipped copy about the given plane [11, 8].

$$S = \frac{\sum_i^w \sum_j^h \sum_k^d I_{ijk}^o I_{ijk}^f}{\sqrt{\left(\sum_i^w \sum_j^h \sum_k^d I_{ijk}^f I_{ijk}^f\right) \left(\sum_i^w \sum_j^h \sum_k^d I_{ijk}^o I_{ijk}^o\right)}} \quad (1)$$

where w , h , d are respectively width, height and depth of the 3D neuroimage, I_{ijk}^o is intensity value of the voxel with coordinates i , j , k in the original image, I_{ijk}^f is intensity value of the voxel with coordinates i , j , k in the flipped image.

After preprocessing, we transform the original neuroimage into a binary edge image. (1) reduces to

$$S = \frac{M}{\sqrt{N \cdot N}} = \frac{M}{N} \quad (2)$$

where N is the total number of non-zero voxels in the binary image, M is the total number of coordinate triples for which voxels in both original and flipped binary neuroimages have non-zero values. The formula (2) suggests that we only need to consider non-zero voxels of the binary edge image, which makes the evaluation process much faster

The algorithm is implemented using Insight Toolkit. Anisotropic diffusion is done using classic Perona-Malik algorithm [12]. Canny edge detection method is used to find edges in the MR images. For the edge detection, threshold of 0.11 and gaussian smoothing filter with variance of 20 mm were used for subsampled image; and threshold of 0.04 and gaussian smoothing filter with variance of 5 mm were used for the original image. The algorithm takes about 7 minutes to complete on a PC with Pentium IV 2.6Ghz processor.

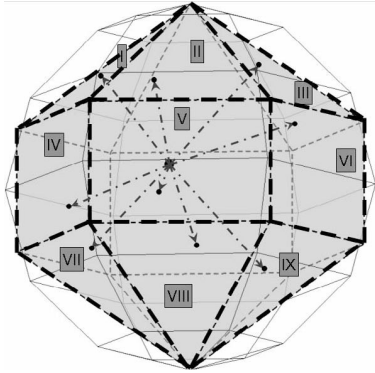


Fig. 2. The figure demonstrates the way we partition the unit hemisphere into sectors and introduces the numbering of the sectors

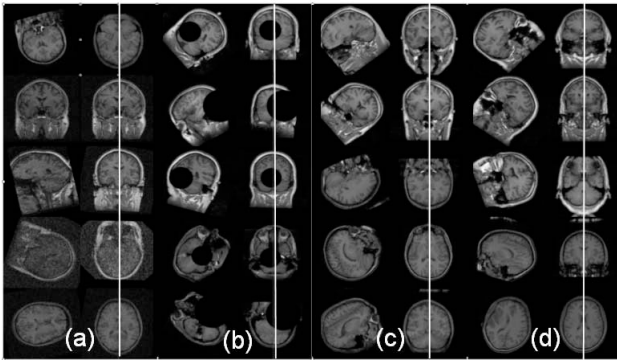


Fig. 3. (a) slices of input and reoriented brain images from *Noise* dataset, (b) -from *Tumor* dataset, (c) - from *Normal* dataset, and (d) - from *Symmetry* dataset.

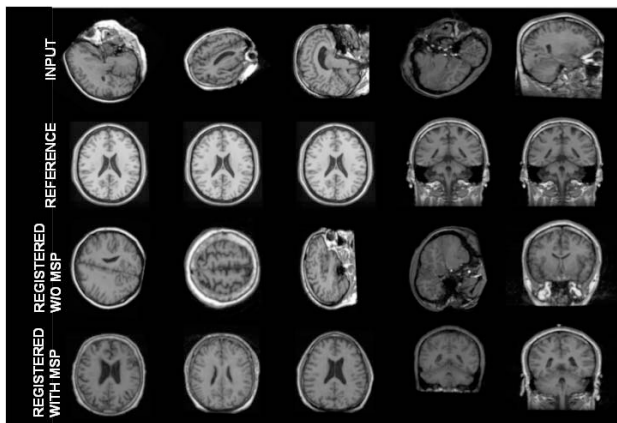


Fig. 4. Advantage of using iMSP for registration. First row contains the slices of input neuroimages. Second row contains slices of the target neuroimage to which we register the input brain image. Third row contains the result of registration without reorienting input brain image according to iMSP. Fourth row contains results of registration after reorientation had been applied.

Table 1. Absolute strength of noise added to each image, in dBW.

Neuroimage #	1, 6, 11, 16	2, 7, 12, 17	3, 8, 13, 18	4, 9, 14, 19	5, 10, 15
Noise, dBW	40	30	20	10	50

Table 2. Parameters of simulated tumors. X, Y, Z are coordinates of the center of a simulated tumor and R is the radius of the tumor, in voxels

Neuroimage #	1, 6, 14, 19	2, 7, 10, 15	3, 8, 11, 16	4, 9, 12, 17	5, 13, 18
X, voxels	100	120	140	160	80
Y, voxels	120	130	140	150	110
Z, voxels	100	100	100	100	100
R, voxels	30	40	50	60	20

4. EVALUATION

In this section we will quantitatively characterize robustness of the proposed iMSP extraction algorithm. As the measure of error of our algorithm we will use angle α , in degrees, between vector normal to true iMSP, \vec{V} , and vector normal to an iMSP estimated by the algorithm, $\vec{\hat{V}}$.

We will test our algorithm on 19 3D MR neuroimages. For convenience, the images were resampled to have cubic voxels and dimensions of $256 \times 256 \times 256$ voxels. We call this dataset *Normal*. Three additional datasets are created based on this *Normal* dataset: *Noise*, *Tumor* and *Symmetric*. Parameters of added noise and simulated tumors are summarized in Tables 1 and 2 respectively. *Symmetric* dataset is created by reflecting left half of every brain in the *Normal* dataset about plane $x = 128$.

In order to evaluate accuracy of the proposed algorithm for arbitrary orientations of the 3D neuroimages, we apply 9 rotations R_i to every volume in each of the four datasets. We choose rotations so that each R_i is random and at the same time the set of R_i is spread out through the entire set of possible rotations. As far as midsagittal plane extraction is concerned, orientation of a volume is defined by the orientation of its iMSP, which, in turn, is defined by \vec{V} . Therefore, we partition the space of orientations of iMSPs into 9 sectors as illustrated by the rightmost sphere in the Figure 2 and ensure that each R_i maps \vec{V} inside a different sector. In such manner we obtain 9 additional volumes for every neuroimage in each of the four datasets. This brings the total number of neuroimages in our entire testing set to $19 \times 4 \times (1 + 9) = 760$. Sample results of our algorithm are presented in the Figure 3

For each image in our test set we know, by construction, the rotation transform R which was applied to it. Since originally midsagittal planes of the neuroimages we chose were approximately parallel to yz -plane, after we run the algorithm on an image in the test set, we obtain estimate E of R^{-1} . We can evaluate quality of this estimate by the angle α between the correct normal vector \vec{V} and the estimated $\vec{\hat{V}}$. For each of the four datasets, for every neuroimage j and orientation i

$$\alpha_{ij} = \cos^{-1} \frac{(E_{ij} R_{ij} [1 \ 0 \ 0]^T) \bullet [1 \ 0 \ 0]^T}{|E_{ij} R_{ij} [1 \ 0 \ 0]^T|} \quad (3)$$

Since in the neuroimages from *Normal*, *Tumor* and *Noise* datasets

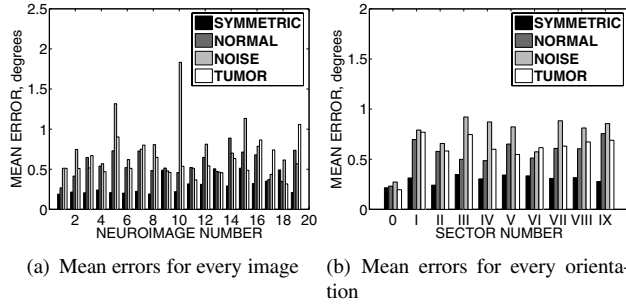


Fig. 5. The graphs show mean errors of the algorithm for (a) every image and every orientation (b).

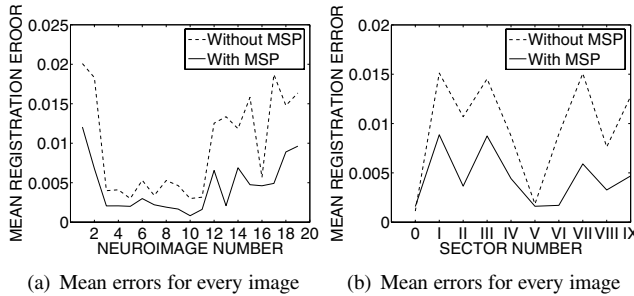


Fig. 6. The graphs show that accuracy of registration is improved for (a) every brain image and (b) every orientation when iMSP extraction algorithm is applied before the registration.

iMSP is only approximately parallel to yz-plane, our results for these images may be biased even if the algorithm works perfectly. To correct for this, for these three datasets, we substitute vector $\begin{bmatrix} 1 & 0 & 0 \end{bmatrix}^T$ in the equation (3) by $0.1 \sum_{i=1}^{10} E_{ij} R_{ij} \begin{bmatrix} 1 & 0 & 0 \end{bmatrix}^T$. Error plots are presented in Figure 5. Our algorithm has mean error of 0.562 degrees when applied to *Normal* dataset; 0.242 degrees when applied to *Symmetric* dataset, and 0.604 and 0.746 degrees when applied to *Tumor* and *Noise* datasets respectively. Our algorithm's accuracy does not suffer from noise or simulated tumors as long as noise strength is less than 50dBW.

5. IMSP AND REGISTRATION

Process of neuroimage registration can benefit from iMSP extraction. First, prealigning two MSPs of two images to be registered helps registration avoid local extrema. Second, by requiring that iMSPs of two registered neuroimages coincide, we reduce the number of parameters a registration procedure has to optimize. In the case of rigid registration, for example, 6 continuous parameters can be reduced to 4: three continuous representing rotation parallel to iMSP and 2 translations, and one binary representing flip. To evaluate advantages for registration provided by our iMSP extraction algorithm, we conducted experiments using 190 neuroimages from *Normal* dataset. We used rigid registration algorithm available in Insight Toolkit [7] with mean intensity square difference as a similarity measure and initialization using moments of inertia turned on. Our experiments have shown that reducing number of degrees of freedom using constraints imposed by iMSP makes registration more than twice as fast compared to mere alignment of iMSPs of two images without sacrificing quality of registration. Our other findings in terms of reliability and accuracy of registration which employs midsagittal plane extraction are presented in Figures 4 and 6.

6. CONCLUSIONS

We have presented a robust truly three dimensional algorithm for ideal midsagittal plane extraction. We have shown that, unlike other existing algorithms, our algorithm has no limitations on the initial orientation of the input neuroimage while achieving accuracy comparable to that of existing algorithms. In addition, we have demonstrated and quantitatively evaluated the improvements in registration accuracy, speed and reliability of neuroimage registration that are made possible by our ideal midsagittal plane extraction algorithm. Although we did extensive evaluation only on MR images, our algorithm should perform well on other image modalities for which edges can be found reliably.

7. REFERENCES

- [1] Ardekani, B., Kershaw, J., Braun, M., and Kanno, I. *Automatic detection of the mid-sagittal plane in 3-d brain images*. IEEE Transactions on Medical Imaging 16(6): 947952, 1997
- [2] Brummer, M. *Hough transform detection of the longitudinal fissure in tomographic head images*. IEEE Transactions on Medical Imaging 10(1): 7481, 1991
- [3] Canny, J. *A Computational approach to edge detection*. IEEE Pattern Analysis and Machine Intelligence, 8(6):679-698, 1986.
- [4] Crow, T. *Schizophrenia as an anomaly of cerebral asymmetry*. In K. Maurer, editor, *Imaging of the brain in psuichiatry and related fields*. Springer-Verlag, 1993.
- [5] Geschwind, N. and Levitsky, W. *Human brain: left-right asymmetries in temporal speech region*. Science, 161:186-187, 1968.
- [6] Guillemaud, R., Marais, P., Zisserman, A., McDonald, T., and Crow, B. *A 3-dimensional midsagittal plane for brain asymmetry measurement*. Schizophrenia Research 18(2-3):183184, 1995
- [7] Ibanez, L., Schroeder, W., Ng, L., Cates, J. *ITK Software Guide* Kitware, Inc., 2003.
- [8] Liu, Y., Collins, R., and Rothfus, W., *Robust Midsagittal Plane Extraction from Normal and Pathological 3-D Neuroradiology Images*, IEEE Transactions on Medical Imaging, 2001.
- [9] Liu, Y. and Dellaert, F. *A classification-based similarity metric for 3D image retrieval*. In Proceedings of Computer Vision and Pattern Recognition Conference, pages 800:805, June 1998.
- [10] Liu, Y., Rothfus, E., and Kanade, T. *Content based 3d neuroradiologic image retrieval: Preliminary results*. IEEE Workshop on Content-Based Access of Image and Video Libraries, in conjunction with International Conference of Computer Vision, pages 91, 100, January 1998.
- [11] Matsuda, T., Yamamoto, K., and Yamada, H. *Detection of partial symmetry using correlation with rotated-reflected images*. Pattern Recognition, 26(8):1245, 1253, 1993.
- [12] P. Perona, J. Malik. *Scale space and edge detection using anisotropic diffusion* Proc. IEEE Comp. Soc. Workshop on Computer Vision, IEEE Computer Society Press, Washington, 16-22, 1987.
- [13] Prima, S., Oursein, S., Ayache, N. *Computation of the mid-sagittal plane in 3-D brain images* IEEE Transactions on Medical Imaging 21(2): 122138, 2002
- [14] Talairach, J. and Tournoux, P. *Co-Planar Stereotaxic Atlas of the Human Brain* Thieme Medical Publishers, 1988.
- [15] Thirion, J., Prima S., and Subsol, G. *Statistical analysis of normal and abnormal dissymetry in volumetric medical images*. In Proceedings of Workshop on Biomedical Image Analysis, pages 74-83. IEEE Computer Society, 1998.